Iranian Journal of Chemical Engineering
Vol. 12, No. 3 (Summer 2015), IAChE

Modification of Montmorillonite and Prediction of Polymer/Clay Affinity Using Surface Properties and Lattice Model

Sh. Mehmandoust[1], M. R. Moghbeli[1*], M. Dadban[1], H. Karimian[2]

[1]School of Chemical Engineering, Iran University of Science and Technology (IUST), Tehran, Iran

[2]School of Chemical Engineering, Golestan University, Gorgan, Iran

Abstract

Sodium montmorillonite (Na-MMT) was organically modified using 11-aminoundecanoic acid (AUA) and methacryloxyethyltrimethylammonium chloride (MAETAC) via cation exchange reaction. The effect of the modifier type and concentration on the structure and surface properties of the organically modified montmorillonites (OMMTs) was investigated. According to the results, the basal spacing of organoclays was enlarged considerably with increasing the AUA concentration, while increasing the MAETAC concentration had no significant influence on OMMT's gallery height. On the other hand, contact angle measurements revealed that increasing the modifiers concentration would increase the hydrophobicity of pristine montmorillonite. The FTIR spectra showed that the OMMTs interlayer environment changed from liquid-like to solid-like as the modifier concentration increased. A mean-field lattice-based model was applied to various polymer/OMMT systems to predict the affinity between the prepared OMMTs and some polymers with different hydrophobicity. The model results showed that high polar and hydrophilic polymers, such as poly(ethylene oxide), exhibit more negative free energy change and stronger interaction with the OMMTs and, consequently, higher potential for preparation of composites with desirable nanostructure and mechanical properties.

Keywords: *Contact Angle, Montmorillonite, Mean-Field Lattice-Based Model, Nanocomposite*

1. Introduction

Polymer/clay nanocomposites offer tremendous improvement in a wide range of physical and engineering properties for polymers with low filler loading [1-4]. However, most polymers are hydrophobic and are not compatible with hydrophilic pristine clay sheets; therefore, it is necessary to modify pristine clay before use in preparation of polymer/clay nanocomposites. Alkylammoniums are the most commonly used organic compounds to modify hydrophilic pristine clay to an organophilic clay material via cation exchange reactions [5-8]. In this case, aliphatic long chains of onium ions with positively charged ends are tethered to the surface of negatively charged silicate layers, resulting in an increase in clay

∗ Corresponding author: mr_moghbeli@iust.ac.ir

gallery height. Intercalating modifier allows polymers or monomers to diffuse within organically modified montmorillonite (OMMT) layers; thereby nanoplatelets would be homogeneously incorporated and distributed in polymeric matrices. On the other hand, the organic cations as OMMT modifier lower the surface free energy of silicate layers and improve their compatibility with hydrophobic polymers [9-15]. In addition, the presence of functional groups or double bonds in the structure of organic modifier may provide the capability of reacting with functionalized polymers or monomers within organoclay galleries [4–8, 16–19]. Moreover, interlayer structure and surface properties of OMMT will strongly influence the resultant microstructure and mechanical properties of polymer/clay nanocomposite. A suitable thermodynamic model can be used to predict the equilibrium state of polymer/clay nanocomposites.

1-1. Thermodynamic model

Vaia and Giannelis [12–15] proposed a lattice-based model for polymer melt intercalation in organically modified clays. Based on this model, the final microstructure of polymer/clay composites prepared by melt intercalation process depends on the free energy change of the system (Δf):

$$\Delta f = f(h) - f(h_0) = \Delta E - T\Delta S \qquad (1)$$

where ΔE, ΔS and T are internal energy change, entropy change and temperature, respectively. h_0 and h are the clay gallery heights before and after melt intercalation, respectively. If $\Delta f < 0$, the layer separation is favorable and intercalation of polymer chains within the clay interlayers occurs more effectively.

The entropy change is described as follows [12]:

$$\Delta S \approx \Delta S_V^a + \Delta S_V^P = N_A k_B \left(\frac{1}{\upsilon_2} \varphi_2 \ln(c)(\chi_s - \chi_{s0}) - \left(\frac{\varphi_1}{\upsilon_1} \frac{\pi}{6} \left(\frac{a_1}{h} \right)^2 + \frac{\varphi_1}{\upsilon_1} \sqrt{\frac{3}{m_1}} u \frac{a_1}{h} \right) \right) \qquad (2)$$

where ΔS_V^a is the entropy gain of the modifier chains in the gallery, ΔS_V^P is the entropy loss in confining an initially unconstrained polymer into the clay interlayer, N_A is Avogadro number, k_B is Boltzmann constant, φ_1 is the volume fraction of polymer, φ_2 is the volume fraction of modifier, and c is a statistical surface factor. The terms v_1, m_1 and a_1 are the molar volume per segment, the number of segments per chain, and the segment length of the polymer, respectively. The term u is the Dolan–Edwards dimensionless excluded volume parameter; χ_{s0} and χ_s are the fractions of interlayer volume next to the clay surface accessible by the organic modifier at h_0 and h, respectively.

The internal energy per interlayer volume ($\Delta E/Vol$) is expressed as follows [12–15]:

$$\frac{\Delta E}{Vol} = \Delta e_v = \varphi_1 \varphi_2 \frac{\left(\frac{2}{h_0} \varepsilon_{sp,sa} + \frac{2}{r_2} \varepsilon_{ap} \right)}{1 - \varphi_2 \left(1 - \frac{r_1}{r_2} - \frac{r_1}{h_0} \right)} \qquad (3)$$

where the terms ε_{jk} are the pairwise interaction energy per area between species j and k expressed as the interfacial energies (γ_{jk}). It can be assumed $\varepsilon_{ap} \approx \gamma_{ap}$ and $\varepsilon_{sp,sa} \approx$

($\gamma_{sp} - \gamma_{sa}$) in which the subscripts *s*, *p* and *a* represent the clay surface, polymer, and organic modifier, respectively. The parameter r_i is the radius of interaction surface. Equations (4-6) describe pairwise dispersive component (γ_{jk}^{d}), polar component (γ_{jk}^{p}), and total interfacial energy (γ_{jk}), respectively [12–15]:

$$\gamma_{jk}^{d} = \left(\sqrt{\gamma_j^{d}} - \sqrt{\gamma_k^{d}}\right)^2 \quad (4)$$

$$\gamma_{jk}^{p} = 2\left(\sqrt{\gamma_j^{+}} - \sqrt{\gamma_j^{-}} - \sqrt{\gamma_k^{-}}\right) \quad (5)$$

$$\gamma_{jk} = \gamma_{jk}^{d} + \gamma_{jk}^{p} \quad (6)$$

where γ^{+} and γ^{-} are electron acceptor and donor character of species, respectively. Dispersive (γ_s^{d}) and polar (γ_s^{p}) components of the surface energy may be obtained by contact angle measurements using the mean-geometric approximation model (MGAM) [20]:

$$\gamma_l\left(1+\cos\theta\right) = 2\left[\left(\gamma_l^{d}.\gamma_s^{d}\right)^{1/2} + \left(\gamma_l^{p}.\gamma_s^{p}\right)^{1/2}\right] \quad (7)$$

where γ_l^{p} and γ_l^{d} are polar and dispersive components of the test liquid, respectively. By plotting $\gamma_l\left(1+\cos\theta\right)/2\left(\gamma_l^{d}\right)^{1/2}$ versus $(\gamma_l^{p}/\gamma_l^{d})^{1/2}$, γ_s^{p} and γ_s^{d} values are obtained from the square of slope and intercept of the resultant linear curve, respectively [20].

The aim of the present work is to predict the potential application of organically modified nanoclays for preparation of polymer/clay nanocomposites via theoretical calculations. For this purpose, the effect of two organic modifiers, 11-aminoundecanoic acid (AUA) and methacryloxyethyltrimethylammonium chloride (MAETAC), on interlayer structure and surface properties of the prepared OMMTs was investigated. The results of contact angle measurements of the OMMTs as surface parameters were used to calculate Helmholtz free energy using original mean-field model. Finally, the mean-field lattice-based model [12] was used to predict the affinity between OMMTs and various polymers, which is a crucial parameter to prepare polymer-based nanocomposites.

2. Experimental

2-1. Materials

All chemical reagents were purchased from Merck Co. (Darmstadt, Germany), unless otherwise stated. CloisiteNa^{+} (Na-MMT) with cation exchange capacity (CEC) of 95 meq/100 g was purchased from Southern Clay Inc., USA. 11-aminoundecanoic acid (AUA) and methacryloxyethyltrimethylammonium chloride (MAETAC) (Fig. 1) as organic modifiers were used without any further purification. Distillated deionized water (DDI) was prepared in the author's laboratory and used as dispersing media. Chloridric acid was utilized to adjust pH. Ethylene glycol (EG), dimethyl formamide (DMF), and DDI were used for contact angle measurements.

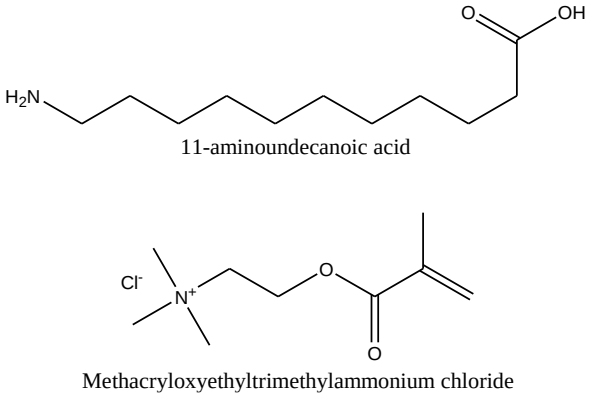

Figure 1. Chemical structure of organic modifiers.

2-2. Clay surface modification

3 g Na-MMT was dispersed in 100 mL DDI, and the suspension was stirred at 400 rpm overnight using a mechanical stirrer to obtain a homogenous dispersion of Na-MMT in water. In a separate beaker, a certain amount of AUA was dissolved in 100 mL DDI and its pH value was adjusted to pH3 using 0.1 M HCl solution to protonize the AUA modifier. The modifier solution was added dropwise to the Na-MMT dispersion, and then the suspension was stirred at room temperature for a further 24 h. The precipitated modified clay was filtered and then washed with HCl solution and DDI several times and was dried in a vacuum oven at 60ºC overnight. A same procedure was used for the MAETAC modification of Na-MMT. In all cases, the modified clays were designated by a code depending upon the modifier type and concentration used to modify the pristine clay, i.e. CloisiteNa$^+$. The code for the OMMT has a general X-*a* form in which X and *a* are the modifier type and the initial concentration of organic modifier, respectively. For instance, AUA-0.75 represents an OMMT in which the concentration of AUA is equal to 0.75 of the CEC of the pristine clay.

2-3. Characterization

Several methods were used to characterize the OMMTs. X-ray diffraction (XRD) experiment was carried out on a Siemens D5000 X-ray diffractometer using Cu Kα (λ=1.542 Å) radiation. The infrared spectra of the OMMT were studied using a Fourier transform infrared (FTIR, Shimadzu, Japan) apparatus. All spectra in the range of 400-4000 cm^{-1} with a 2 cm^{-1} spectral resolution were obtained from compressed KBr pellets containing the OMMT samples. Contact-angle measurements were carried out using three test liquids including water, ethylene glycol (EG), and dimethyl formamide (DMF) on the OMMT disks prepared by compression molding. For this purpose, dry OMMT powder was molded in a stainless steel mold 25 mm in diameter under 2500 psi load. The OMMT disk specimens were stored in a vacuum desiccator for 24 h before use. The thermal stability and presence of AUA molecules inside the silicate layers were investigated by thermal gravimetric analysis (TGA) instrument under nitrogen atmosphere in the temperature range of 25-600°C.

3. Results and discussion

3-1. OMMT nanostructure

The CloisiteNa$^+$ was modified with various modifier concentrations below and above its cation exchange capacity (CEC) ranging from 0.75 to 3 CEC. Fig. 2a shows the XRD patterns of CloisiteNa$^+$ and its modified structures with various AUA modifier concentrations. The basal spacing of the neat and modified clays was calculated using the Bragg's equation as listed in Table 1. The basal spacing of 1 nm for the Na-MMT obtained from XRD

analysis is consistent with that value reported by other researchers showing a difference of ±5% [22]. In addition, the XRD patterns indicated that the basal spacing of the AUA-modified clay increased from 13.61 to 21.75 Å with increasing the AUA concentration from 0.75 to 3 CEC. Upon increasing the aqueous modifier concentration up to 1.5 CEC, the 2θ-maximum peak considerably shifted from a higher angle (2θ=8.33°), corresponding to a basal spacing of 10 Å, to a lower angle (2θ=4.32°) with a higher basal spacing of 20.44 Å. Nevertheless, further increase in AUA concentration did not lead to significant basal spacing enlargement (Table 1). When the AUA concentration in the aqueous solution is close to the CEC of the pristine clay, the organic modifier molecules react with the clay interlayer cations effectively and saturate the pristine clay. Beyond the CEC concentration, the intercalation of organic modifier is limited due to steric hindrance of pre-intercalated species. Therefore, the basal spacing of the organoclays increases slightly for modifier concentrations above 1.5 CEC. The broadening of half width of the maximum peaks indicates a heterogeneous modifier intercalation within the OMMT galleries, especially at higher AUA concentrations (Fig. 2a). In addition, the increase of the modifier concentration from 0.75 to 3 CEC may vary the AUA molecules arrangement from lateral-monolayer to lateral-bilayer or paraffin-type monolayer in the interlayer region (Fig. 3) [21]. The small energy difference between the *trans* and the *gauche* conformation of the modifier alkyl chains allows a great degree of conformational freedom for the alkyl chain tail of the AUA molecules tethered on OMMT layers and confined inside the galleries [22].

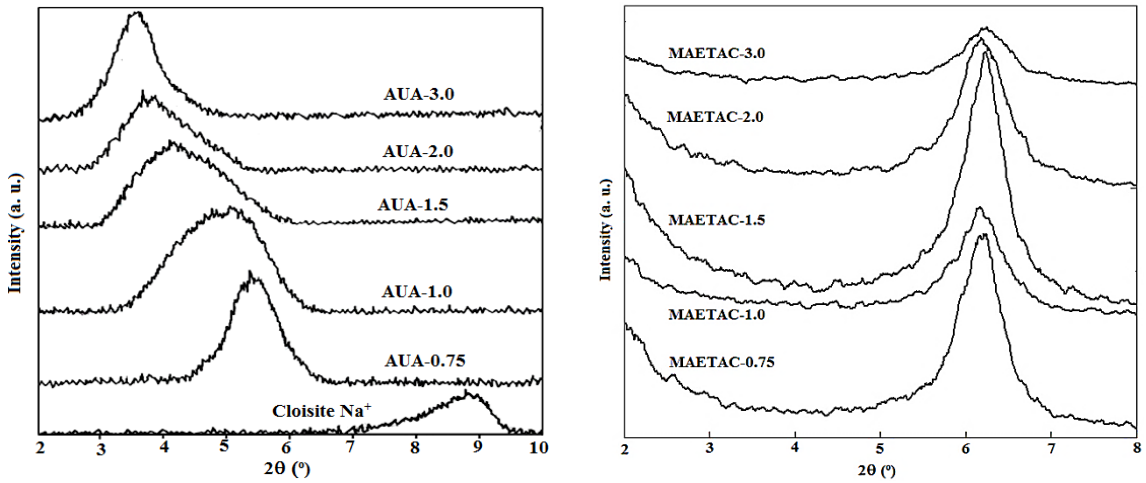

Figure 2. (a) X-ray diffraction patterns of organoclays modified with various content of (a) AUA and (b) MAETAC

Table 1
The analysis of XRD patterns and surface energies of organo-modified clays.

Organoclay	2θ (°)	d-spacing (Å)	γ^d (mJ/m^2)	γ^p (mJ/m^2)	γ^+ (mJ/m^2)	γ^- (mJ/m^2)	γ^{total} (mJ/m^2)
Na-MMT[a]	8.83	10.00	660.5	10.04	0.70	36.01	76.04
AUA-0.75	6.49	13.61	13.13	44.88	6.67	49.99	58.01
AUA-1.0	6.06	14.57	12.97	44.13	5.97	51.17	57.10
AUA-1.5	4.32	20.44	13.81	40.21	5.20	47.46	54.02
AUA-2.0	4.20	21.02	15.12	35.09	4.39	41.98	50.21
AUA-3.0	4.06	21.75	19.46	23.12	3.08	26.97	42.58
MAETAC-0.75	6.19	14.27	17.85	31.17	5.97	30.69	49.02
MAETAC -1.0	6.14	14.38	16.94	32.90	3.57	40.17	49.84
MAETAC -1.5	6.55	14.25	16.94	32.90	3.57	40.17	49.84
MAETAC -2.0	6.13	14.41	15.58	32.65	6.85	30.53	48.23
MAETAC -3.0	6.30	14.01	19.10	23.28	6.02	19.11	42.38

*. [a] Na-MMT, non-modified clay values, are taken from literature [14].

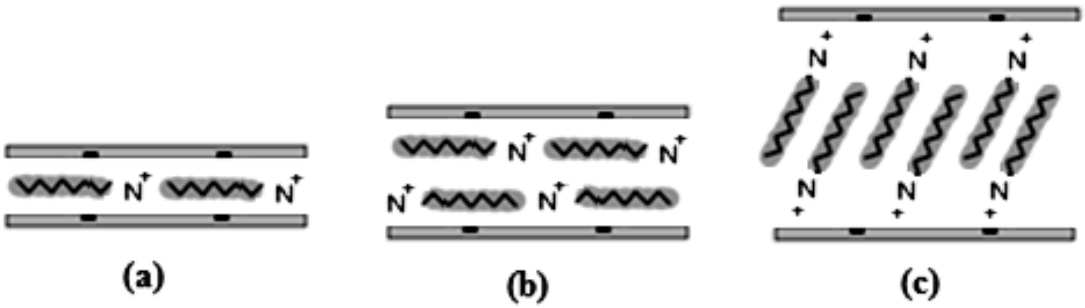

Figure 3. Orientations of modifier molecules in the nanoclay galleries; (a) lateral-monolayer, (b) lateral-bilayer, and (c) paraffin-type monolayer arrangements

Fig. 2b shows X-ray patterns of the CloisiteNa$^+$ modified with various MAETAC modifier concentrations. As shown in Table 1, the basal spacing increase of OMMTs with increasing the MAETAC concentration is much lower than that of the AUA-modified clay. This behavior can be attributed to the lower affinity of MAETAC molecules to penetrate into the clay interlayer region as compared with the AUA molecules. On the other hand, the maximum peaks did not shift significantly to lower angles and the gallery height was almost constant with increasing the MAETAC concentration (Table 1 and Fig. 2). However, the high intensity of MAETAC-modified clays in the X-ray patterns confirms a high level of ordered lamellar stacking in the modified clay [23]. In this case, the maximum gallery height was achieved when the modifier concentration increased to 2 CEC. Further increase in modifier concentration slightly decreased the basal spacing presumably due to the steric restriction of pre-intercalated MAETAC molecules.

Although the intercalation of the modifiers into MMT galleries was investigated by XRD analysis, the selected TGA of the AUA-modified clays (Fig. 4) exhibited the presence of more AUA

molecules between the silicate layers, and consequently a higher basal spacing of the OMMTs, with increasing the AUA concentration. Fig. 4 indicates the TGA curves for the modified clays with various AUA contents. As shown, a small amount of weight loss, 1.5-3%, was observed in the temperature range of 40–140°C due to the evaporation of water of hydration in the modified clays. Table 3 summarized the TGA results of the AUA-modified clay specimens. A significant weight loss in the organically modified clay above 140°C was observed due to the decomposition of the intercalated AUA modifier inside the galleries. The 1 CEC AUA-modified clay exhibited the highest thermal stability and decomposition temperature of 354.1°C, while the modified clay with the highest modifier content, i.e. 4 CEC, showed the lowest thermal stability or decomposition temperature. As expected, the loss weight increased with increasing AUA content inside the galleries (Table 3).

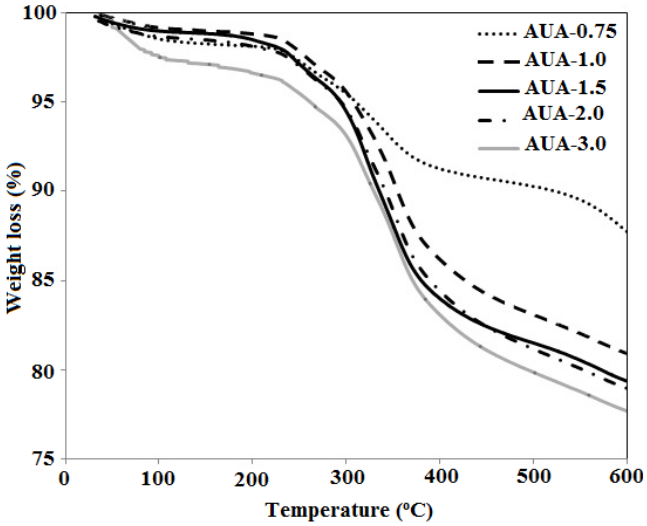

Figure 4. TGA of the modified Na-MMT with various AUA contents.

Table 2
TGA results of the modified clays with various AUA modifier content.

Organoclay	CEC	T_1^* (°C)	Loss weight (%)	T_2^* (°C)	Loss weight (%)
AUA-0.75	0.75	74.3	2.2	325.6	9.6
AUA-1.0	1.00	68.6	1.8	354.1	17.5
AUA-1.5	1.50	64.5	1.3	345.5	18.9
AUA-2.0	2.00	61.9	1.6	346.8	20.2
AUA-3.0	4.00	54.8	2.9	336.9	22.6

* T_1 and T_2 are the first and second decomposition temperatures with the highest rate of loss weight.

3-2. Surface properties of OMMTs

To evaluate the Helmholtz free energy by the lattice-based mean-field model [12], only surface free energies should be evaluated. For this purpose, contact angle test was used to measure the surface free energies of the organically modified Na-MMTs (OMMTs). The surface properties of the OMMTs were determined by contact angle measurements. The polar and dispersive components of the surface free energy were calculated using the mean geometric approximation model (MGAM) [20]. Table 1 shows the surface energies of the modified clays. Upon increasing the AUA concentration in the modifier solution from 0.75 to 3 CEC, the total surface free energy of the pristine clay decreased from 76.04 to 42.58 mJ/m^2, while the polar component of surface energy (γ^p) increased to some extent. The intercalated AUA molecules with a nonpolar aliphatic chain tail and hydrophobic nature would improve the affinity of polymer chains to diffuse into the modified silicate layers. In other words, the decrease of clay surface free energy enhances the polymer/clay compatibility and facilitates the clay delamination in polymeric matrix. Increasing the AUA concentration up to 1.5 CEC significantly lowered the surface free energy, while further modifier addition slightly decreased the surface free energy. This behavior can be attributed to saturation of cation exchange capacity (CEC) of the clay at AUA concentrations above 1.5 CEC. At higher AUA concentrations, although the modifier molecules penetrate further into the galleries (Fig. 3), the included modifier molecules could not tethered effectively on the surface of silicate layers.

The surface free energies of the clay modified with various MAETAC levels are shown in Table 1. The higher nonpolar character of MAETAC could enhance the hyrophobicity of the silicate layers more than the AUA molecules. On the other hand, the MAETAC molecule with a C=C end double bond (Fig. 1) may be polymerized with the intercalated monomers inside the galleries. Therefore, this improves OMMT delamination inside polymer matrix; thereby enhancing the physical and mechanical properties of the reinforced polymers [16–19]. According to contact angle measurements, increasing MAETAC concentration from 0.75 to 3 CEC, the dispersive component of the surface free energy increased from 17.85 to 19.11 mJ/m^2, while the polar component decreased from 31.17 to 23.29 mJ/m^2. Nevertheless, the total surface energy of the clay slightly decreased as the modifier concentration increased. This is indicative of increased hydrophobic character of the MAETAC-modified clays. However, the surface free energy changes are not very sensitive to MAETAC concentration (Table 1). This may be due to lower affinity of the MAETAC molecules to silicate layers in comparison with the AUA molecules.

3-3. Molecular conformation of modifier

The molecular conformation of the intercalated modifier chains was studied by FTIR spectroscopy. Fig. 5 shows the FTIR spectra of the AUA-modified and MAETAC-modified clays. In the AUA-modified clay, the strongest aliphatic absorption bands observed between 2800 and 3000 cm^{-1} correspond to symmetric and asymmetric stretch vibrations of methylene

(CH_2), respectively. In the case of MAETAC modifier, the absorption bands of methylene and methyl groups appear in the wavenumber range of 2800-3000 cm^{-1}. The phase state of modifier in the interlayer region can be characterized using the FTIR frequency shift method. In general, the frequency of asymmetric stretch vibration of CH_2 ($\nu_{as}(CH_2)$) is sensitive to gauche/trans conformer ratio along aliphatic chain. Lower frequencies are characteristic of highly ordered all-trans conformations and the solid-like interlayer environment. On the contrary, higher frequencies of $\nu_{as}(CH_2)$ vibration are indicative of dominant gauche conformations along hydrocarbon chain and the liquid-like interlayer structure [20-21,24–26]. The frequency of the $\nu_{as}(CH_2)$ vibration as a function of the modifier concentration is shown in Fig. 5c. The increase of modifier concentration and interlayer packing density shifted the frequency of $\nu_{as}(CH_2)$ from 2927 to 2921 cm^{-1} for the AUA-modified clays, while the frequency shifted from 2939 to 2933 cm^{-1} for the MAETAC-modified clays. At low modifier concentration and lower packing density of the modifier molecules, there is no significant frequency shift and no longer fully stretched chains in an all-trans conformation. In fact, the tethered modifier molecules progressively adopt a more disordered structure leading to a more *liquid-like* state (Fig. 3a–b). However, increasing the modifier concentration increased the chain order with more efficient packing and enhanced interchain contacts. In this case, higher cohesive van der Waals interaction between the chains resulted in a solid-like interlayer structure (Fig. 3c).

3-4. Polymer melt intercalation: model predictions

According to the thermodynamic model, the entropy loss associated with polymer confinement inside the clay gallery and the entropy gain associated with the conformation freedom of the modifier chains result in a net entropy change near or slightly below zero. Thus, the morphology of the nanocomposite via melt intercalation depends primarily on the changes in total internal energy [14]. The surface free energy components of various polymeric matrices with different hydrophobicity, including polypropylene (PP), polystyrene (PS), poly(methyl methacrylate) (PMMA), poly(ethylene oxide) (PEO), and nylon 612 are summarized in Table 2. Figs. 6–7 show the model predictions for polymeric nanocomposites, which would be prepared via melt-intercalation using AUA-3.0 and MAETAC-3.0 modified clays. As the dispersive (γ^d) and the electron donor (γ^-) components of the polymer's surface energy increase, the free energy change becomes more negative for the resulting polymer/OMMT system. However, the free energy change is more negative for AUA-3.0 modified clay. The higher γ^- value of the AUA-3.0 modified clay compared to the MAETAC-3.0 modified clay (Table 1) leads to a more effective enthalpic interaction of the modified clay with the intercalated polymer chains, which in turn results in more negative free energy change. Among selected polymers, the PEO exhibited the most negative free energies, about four and seven times greater than the PP with the same modified clays, respectively. This result

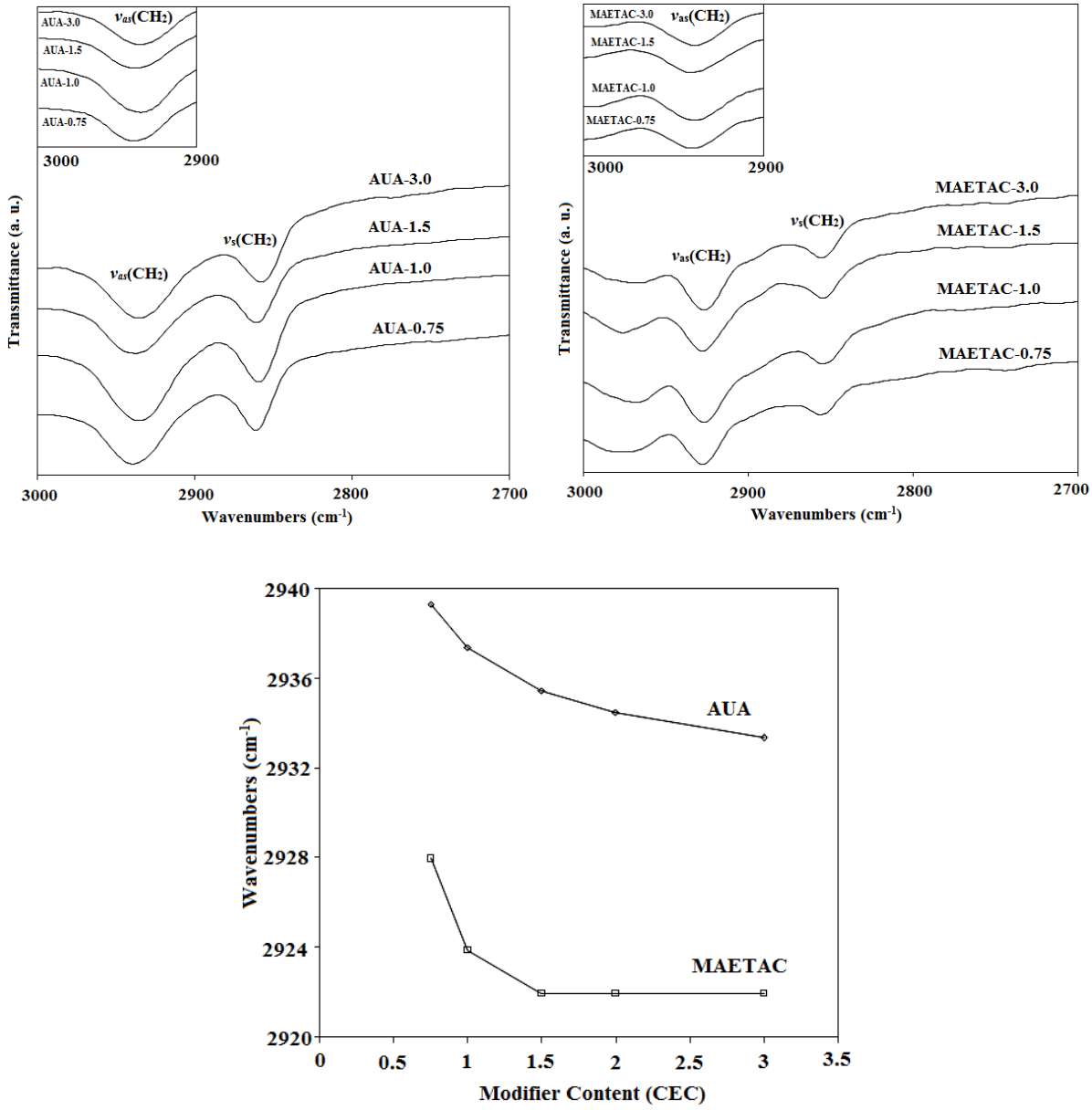

Figure 5. Selected regions of FTIR spectra of organoclays with different modifier content; (a) AUA, (b) MAETAC and (c) $\nu_{as}(CH_2)$ as a function of modifier concentration.

indicates that the PEO chains show the strongest driving force to enter inside the modified clays compared with other selected polymers. In addition, it suggests that the PEO/clay composite system may reach to an exfoliated nanostructure. On the other hand, in the case of nylon 612, the interaction parameter ε_{ap} is positive for both AUA-3.0 and MAETAC-3.0 modified clays (Figs. 6–7b). Accordingly, the calculated free energy change is positive for both cases, although it is slightly lower when the AUA-3.0 modified clay was used as reinforcement. Consequently, it might be expected that the nylon 612 and the modified clays do not have proper affinity to nanocomposite preparation; thereby the resultant polymeric composite would be incompatible in equilibrium state. However, in the thermodynamic model for total interfacial energy, H-bonding

component has not been considered for various MMTs and polymers. This component may play a significant role in the case of MAETAC as well as in the PMMA and Nylon 612. Obviously, any modification to the original lattice-based model to include the contributions of H-bonding and other ignored influential parameters requires much theoretical efforts and would be considered in other future research works.

Fig. 8 shows model predictions for melt intercalation of PS with AUA- and MAETAC-modified clays. γ^{d}, γ^{+} and γ^{-} values for PS are 42.0, 0.0 and 1.1 mJ/m^2, respectively. The change in the free energy becomes more negative when the AUA concentration increases from 0.75 to 3 CEC. The favorite melt intercalation of polystyrene indicates that the composite system would tend to get an exfoliation structure at higher modifier level (Fig. 8a). In the case of MAETAC, the free energy change becomes more negative as the modifier content reaches to 1.5 CEC. However, further increase of MAETAC concentration increases free energies to some extent. In this case, the modified clay prepared with initial MAETAC concentration of 1.5 CEC will presumably provide the best condition for the preparation of PS/OMMT nanocomposite via melt intercalation (Fig. 8b).

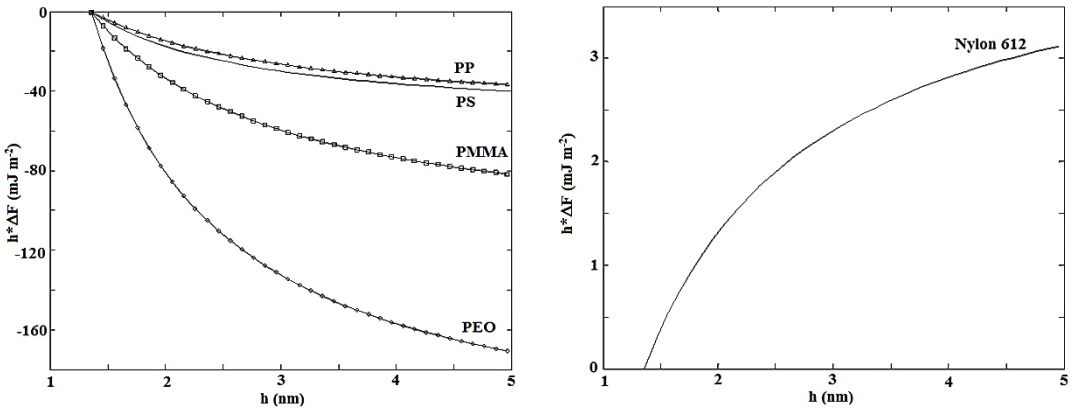

Figure 6. Free energy change calculated for selected polymers/AUA-3.0 nanocomposites as a function of gallery height h.

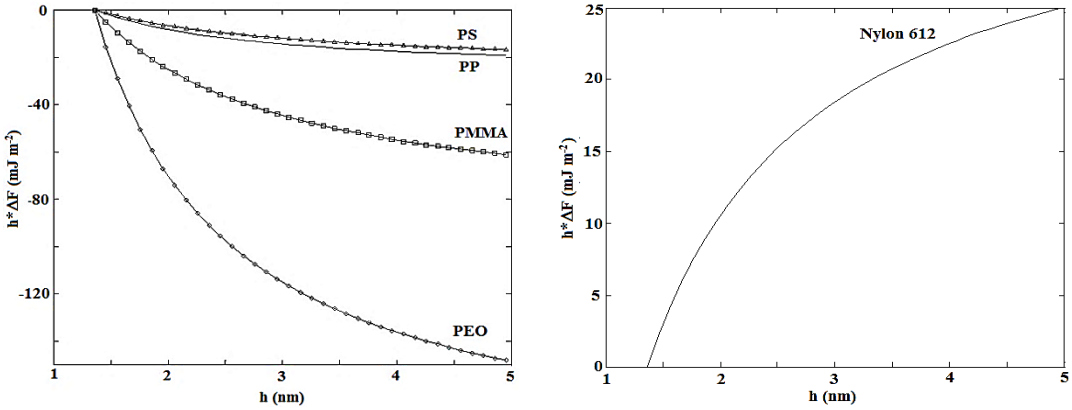

Figure 7. Free energy change calculated for selected polymers/MAETAC-3.0 nanocomposites as a function of gallery height h.

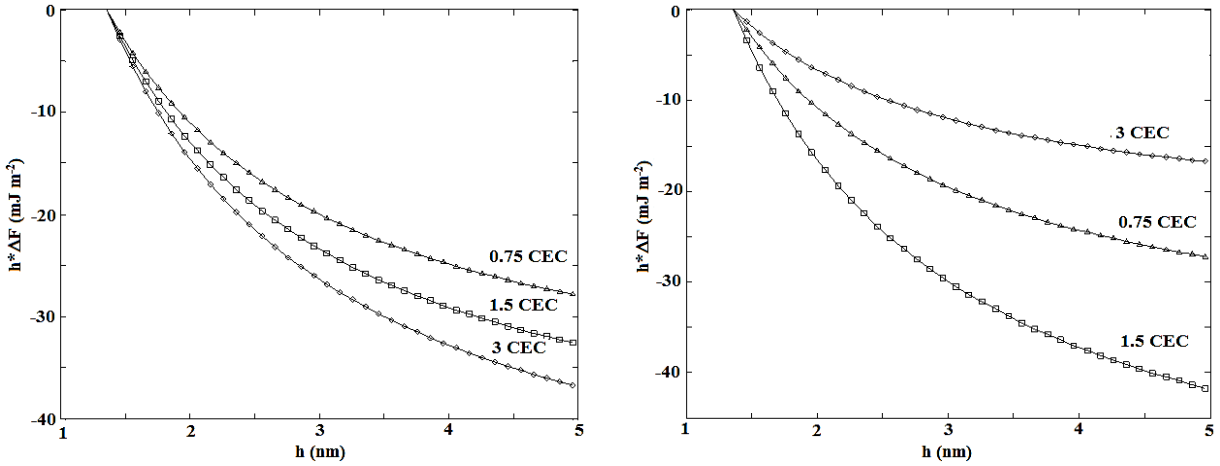

Figure 8. Free energy change calculated for polystyrene nanocomposites with (a) AUA and (b) MAETAC organoclays as a function of gallery height h.

4. Conclusions

Pristine clay was successfully modified with various concentrations of 11-aminoundecanoic acid (AUA) and methacryloxyethyltrimethylammonium chloride (MAETAC) as organic modifiers. The X-ray diffraction analysis showed that increasing the AUA concentration resulted in higher basal spacing of the OMMTs. The basal spacing increase of the MAETAC-modified clays was much lower than that of the clays modified with AUA. This behavior can be attributed to the lower affinity of MAETAC molecules to diffuse into the OMMT interlayer region as compared with the AUA molecules. The contact angle measurements revealed that the inserted organic modifier molecules with aliphatic chains enhanced the hydrophobic nature of OMMTs, thereby the compatibility of the clay layers with the polymer matrix would increase. FTIR spectra confirmed that the molecular conformation of intercalated modifier chains is a function of modifier concentration. As the modifier content increased, the interlayer environment exhibited a *solid-like* structure. At low modifier concentrations, higher gauche/trans ratio conformation resulted in a *liquid-like* structure. The thermodynamic model predictions revealed that the high polar and hydrophilic polymers such as PEO show a more negative free energy change and stronger interaction with the OMMTs. This suggests higher potential of high polar hydrophilic polymers for preparation of polymer/AUA or MAETAC nanocomposites via polymer melt intercalation.

References

[1] LeBaron, P. C. Wang, Z. and Pinnavaia, T., "Polymer-layered silicate nanocomposites an overview", *Appl. Clay Sci*., **15**, 11 (1999).

[2] Paul, D. R. and Robeson, L. M., "Polymer nanotechnology: nanocomposites", *Polymer*, **49**, 3187 (2008).

[3] Bousmina, M., "Study of intercalation and exfoliation processes in polymer nanocomposites", *Macromolecules*,

39, 4259 (2006).

[4] Mitall, V., "Polymer chains grafted "to" and "from" layered silicate clay platelets", *J. Colloid Interface Sci*., **314**, 141 (2007).

[5] Zhang, X. Yang, G. and Lin, J., "Crystallization behavior of nylon 11/montmorillonite nanocomposites under annealing", *J. Appl. Polym. Sci*., **102**, 5483 (2006).

[6] Han, B. Ji, G. Wu, S. and Shen, J., "Preparation and characterization of nylon 66/montmorillonite nanocomposites with co-treated montmorillonites", *Eur. Polym. J*., **39**, 1641 (2003).

[7] Shim, J. H. Kim, E. S. Joo, J. H. and Yoon, J. S., "Properties and morphology of poly(L-lactide)/clay composites according to the clay modification", *J. Appl. Polym. Sci.*, **102**, 4983 (2006).

[8] Zhang, X. Yang, G. and Lin, J., "Synthesis, rheology, and morphology of nylon-11/layered silicate Nanocomposite", *J. Polym. Sci. Part B: Polym. Phys*., **44**, 2161 (2006).

[9] Paiva, L. C. Morales, A. N. and Diaz, F., "Organoclays: properties, preparation and applications", *Appl. Clay Sci.*, **42**, 8 (2008).

[10] Fischer, H., "Polymer nanocomposites from fundamental research to specific applications", *Mater. Sci. Eng. C*, **23**, 763 (2003).

[11] Pavildou, S. and Papaspyrides, C. D., "A review on polymer–layered silicate nanocomposites", *Prog. Polym. Sci*., **33**, 1119 (2008).

[12] Vaia, R. A. and Giannelis, E. P. "Lattice model of polymer melt intercalation", *Macromolecules*, **30**, 7990 (1997).

[13] Vaia, R. A. and Giannelis, E. P., "Polymer melt intercalation in organically-modified layered silicates: model predictions and experiment", *Macromolecules*, 30, 8000 (1997).

[14] Ophir, A. Zonder, L. and Rios, P. F., "Thermodynamic characterization of hybrid polymer blend systems", *Polym. Eng. Sci.*, **49**, 1168 (2009).

[15] Meneghetti, P. and Qutubuddin, S., "Application of mean-field model of polymer melt intercalation in organo-silicates for nanocomposites", *J. Colloid Interface Sci.*, **288**, 387 (2005).

[16] Huang, X. and Brittain, W., "Synthesis and characterization of PMMA nanocomposites by suspension and emulsion polymerization", *Macromolecules*, **34**, 3255 (2001).

[17] Xie, S. Zhang, S. and Wang, F., "Synthesis and characterization of poly(propylene)/montmorillonite nanocomposites by simultaneous grafting-intercalation", *J. Appl. Polym. Sci.*, **94**, 1018 (2004).

[18] Herrera, N. Putaux, J. and Lami, E., "Synthesis of polymer/laponite nanocomposite latex particles via emulsion polymerization using silylated and cation-exchanged laponite clay platelets", Prog. Solid State Chem., **34**, 121 (2006).

[19] Qutubuddin, S. Fu, X. and Tajuddin, Y., "Synthesis of polystyrene-clay nanocomposites via emulsion polymerization using a reactive surfactant", *Polym. Bull*., **48**,

143 (2002).

[20] Bouali, B. Ganachaud, F. Chapel, J. P. Pichot, C. and Lanteri, P., "Acid-base approach to latex particles containing specific groups based on wettability measurements", *J. Colloid Interface Sci.*, **208**, 81 (1998).

[21] Zhu, J. He, H. Zhu, L. Wen, X. and Deng, F., "Characterization of organic phases in the interlayer of montmorillonite using FTIR and 13C NMR", *J. Colloid Interface Sci*., **286**, 239 (2005).

[22] Vaia, R. A. Teukolsky, R. K. and Giannelis, E. P., "Interlayer structure and molecular environment of alkylammonium layered silicates", *Chem. Mater*., **6**, 1017 (1994).

[23] Tiwari, R. R. Khilar, K. C. and Natarajan, U., "Synthesis and characterization of novel organo-montmorillonites", *Appl. Clay Sci*., **38**, 203 (2008).

[24] He, H. Ray, F. L. and Zhu, J., "Infrared study of HDTMA+ intercalated montmorillonite", *Spectrochimica Acta A*, **60**, 2853 (2004).

[25] Vasquez, A. Lopez, M. Kortaberria, G., Martin, L. and Mondragon, I., "Modification of montmorillonite with cationic surfactants thermal and chemical analysis including CEC determination", *Appl. Clay Sci*., **41**, 24 (2008).

[26] Xi, Y. Ray, F. L. and He, H., "Modification of the surfaces of Wyoming montmorillonite by the cationic surfactants alkyl trimethyl, dialkyl dimethyl, and trialkyl methyl ammonium bromides", *J. Colloid Interface Sci*., **305**, 150 (2007).